Annals of Botany **124**: 947–960, 2019
doi: 10.1093/aob/mcy242, available online at www.academic.oup.com/aob

ANNALS OF BOTANY
Founded 1887

SPECIAL ISSUE ON ROOT TRAITS BENEFITTING CROP PRODUCTION IN ENVIRONMENTS WITH LIMITED WATER AND NUTRIENT AVAILABILITY

CBL-INTERACTING PROTEIN KINASE 9 regulates ammonium-dependent root growth downstream of *IDD10* in rice (*Oryza sativa*)

Yuan Hu Xuan[1,*], Vikranth Kumar[2,†], Xiao Han[3,†], Sung Hoon Kim[2], Jin Hee Jeong[2], Chul Min Kim[2], Yue Gao[1] and Chang-deok Han[2,*]

[1]College of Plant Protection, Shenyang Agricultural University, Dongling Road 120, Shenyang, 110866 China, [2]Division of Applied Life Science (BK21 Program), Plant Molecular Biology and Biotechnology Research Center (PMBBRC), Gyeongsang National University, Jinju 52828, Korea and [3]College of Biological Science and Engineering, Fuzhou University, Fuzhou, 350108 China

**For correspondence. E-mails: xuanyuanhu115@syau.edu.cn or cdhan@gnu.ac.kr*

[†]These authors contributed equally to this work.

Received: 3 October 2018 Returned for revision: 5 November 2018 Editorial decision: 21 December 2018 Accepted: 2 January 2019
Published electronically 31 January 2019

• **Background and Aims** *INDETERMINATE DOMAIN 10* (*IDD10*) is a key transcription factor gene that activates the expression of a large number of NH_4^+-responsive genes including *AMMONIUM TRANSPORTER 1;2* (*AMT1;2*). Primary root growth of rice (*Oryza sativa*) *idd10* mutants is hypersensitive to NH_4^+. The involvement of *CALCINEURIN B-LIKE INTERACTING PROTEIN KINASE* (*CIPK*) genes in the action of *IDD10* on NH_4^+-mediated root growth was investigated.
• **Methods** Quantitative reverse transcription–PCR was used to analyse NH_4^+- and *IDD10*-dependent expression of *CIPK* genes. *IDD10*-regulated *CIPK* target genes were identified using electrophoretic mobility shift assays, chromatin immunoprecipitation and transient transcription assays. Root growth rate, ammonium content and ^{15}N uptake of *cipk* mutants were measured to determine their sensitivity to NH_4^+ and to compare these phenotypes with those of *idd10*. The genetic relationship between *CIPK9 OX* and *idd10* was investigated by crosses between the *CIPK9* and *IDD10* lines.
• **Key Results** *AMT1;2* was overexpressed in *idd10* to determine whether NH_4^+-hypersensitive root growth of *idd10* resulted from limitations in NH_4^+ uptake or from low cellular levels of NH_4^+. High NH_4^+ levels in *idd10/AMT1;2 OX* did not rescue the root growth defect. Next, the involvement of *CIPK* genes in NH_4^+-dependent root growth and interactions between *IDD10* and *CIPK* genes was investigated. Molecular analysis revealed that *IDD10* directly activated transcription of *CIPK9* and *CIPK14*. Expression of *CIPK8*, *9*, *14/15* and *23* was sensitive to exogenous NH_4^+. Further studies revealed that *cipk9* and *idd10* had almost identical NH_4^+-sensitive root phenotypes, including low efficiency of $^{15}NH_4^+$ uptake. Analysis of plants containing both *idd10* and *CIPK9 OX* showed that *CIPK9 OX* could rescue the NH_4^+-dependent root growth defects of *idd10*.
• **Conclusions** *CIPK9* was involved in NH_4^+-dependent root growth and appeared to act downstream of *IDD10*. This information will be useful in future explorations of NH_4^+ signalling in plants.

Key words: Rice (*Oryza sativa*), ammonium, root growth, *CIPK9*, *IDD10*, transcription factor.

INTRODUCTION

Nitrate (NO_3^-) and ammonium (NH_4^+) are the major forms of nitrogen (N) in higher plants. Nitrogen is an important macroelement required for the synthesis of cellular molecules such as amino acids and nucleotides. Reduction of NO_3^- to NH_4^+ consumes 12–26 % of photosynthetically generated reductant (Patterson *et al.*, 2010), which makes NH_4^+ an energetically favourable N source. At high concentrations, however, NH_4^+ is toxic to many plant species (Britto and Kronzucker, 2002). Rice grown in paddy fields uses NH_4^+ as its main N source. Previous studies on the effects of NH_4^+ on rice seedling roots showed that high NH_4^+ concentrations induce primary root coiling under light conditions, and that inhibition of NH_4^+ assimilation rescues NH_4^+-induced root coiling (Hirano *et al.*, 2008; Shimizu *et al.*, 2009); however, the details of this mechanism remain elusive. We showed previously that *INDETERMINATE DOMAIN 10* (*IDD10*) regulates NH_4^+-mediated gene expression and root growth in rice (*Oryza sativa*) (Xuan *et al.*, 2013); *idd10* mutants are sensitive to NH_4^+ and exhibit short primary roots.

A comparison of the effects of NO_3^- and NH_4^+ on the arabidopsis (*Arabidopsis thaliana*) transcriptome found that approx. 60 % of genes displayed a common response to NO_3^- and NH_4^+. In addition, application of methionine sulphoximine (MSX), an inhibitor of glutamine synthetase, did not block all NH_4^+-responsive genes, indicating that NH_4^+ itself is a signalling molecule (Patterson *et al.*, 2010). Researchers have studied global gene expression changes under N starvation conditions to explore N signalling in rice (Lian *et al.*, 2006; Cai *et al.*, 2012; W. Yang *et al.*, 2015) and a broad range of early responses have been analysed under different concentrations of NH_4^+ (Xuan *et al.*, 2013; S.Y. Yang *et al.*, 2015). Rice genes responding to cellular N status are involved in diverse aspects of metabolism

and signalling, including N and carbon metabolism, stress responses and hormonal signalling, suggesting that NH_4^+ is a signalling molecule that regulates diverse biological pathways in plants.

Expression of the *CALCINEURIN B-LIKE INTERACTING PROTEIN KINASE* 23 (*CIPK23*) gene is sensitive to exogenous NO_3^- content; moreover, in arabidopsis, *CIPK23* interacts with and phosphorylates *NO_3^- TRANSPORTER 1.1* (*NRT1.1*), thus modulating its affinity for its substrate (Ho *et al.*, 2009). Furthermore, when the exogenous NH_4^+ concentration is high, the T460 residue in *AMMONIUM TRANSPORTER 1;1* (*AMT1;1*) is phosphorylated (Lanquar *et al.*, 2009). This reaction is also mediated by *CIPK23* in arabidopsis (Straub *et al.*, 2017); furthermore, *CIPK23* directly regulates the potassium transporter, AKT1, via phosphorylation in both arabidopsis and rice (Xu *et al.*, 2006; Li *et al.*, 2014). Another member of this kinase gene family, *CIPK8*, regulates the low-affinity phase N response (Hu *et al.*, 2009). In arabidopsis, *CIPK9* regulates potassium homeostasis under low potassium conditions (Pandey *et al.*, 2007; Liu *et al.*, 2012). Transcriptomic and phosphoproteomic studies have revealed that transcription and phosphorylation of CIPKs are upregulated during NH_4^+ response (Patterson *et al.*, 2010; Engelsberger and Schulze, 2012), indicating that *CIPK* and nutrient signalling are closely connected in plants.

We explored NH_4^+-dependent root growth using *idd10* mutants, whose roots are hypersensitive to NH_4^+. The relationship between the cellular NH_4^+ level and *IDD10* was examined by overexpressing *AMT1;2* in *idd10* plants. Involvement of *CIPK* genes in NH_4^+-dependent root growth and the interaction between *IDD10* and *CIPK* genes was analysed using quantitative reverse transcription–PCR (qRT–PCR), chromatin immunoprecipitation (ChIP), electrophoretic mobility shift assay (EMSA) and transient transcription assays. Ammonium-dependent root growth was compared between *cipk9* and *idd10* mutants, and, in addition, the genetic relationship between *CIPK9* and *IDD10* was examined. These approaches enabled elucidation of the interaction and relationship between *IDD10* and *CIPK9* in determining NH_4^+-dependent root growth. This constitutes an important contribution to the current understanding of NH_4^+ signalling in plants.

MATERIALS AND METHODS

Plant materials and growth conditions

To examine the effects of NH_4^+ on gene expression, germinated seeds were grown in dH_2O in a greenhouse for 14 d to deplete nutrients in the endosperm. Seedlings were then grown for an additional 3 d in N-free nutrient (–N) solution (Abiko *et al.*, 2005) before being transferred to the same nutrient solution containing 0.5 mM $(NH_4)_2SO_4$. The N-free nutrient solution contained 7 μM $Na_2HPO_4{\cdot}12H_2O$, 16 μM KCl, 7 μM $CaCl_2{\cdot}2H_2O$, 15 μM $MgCl_2{\cdot}6H_2O$, 36 μM $FeSO_4{\cdot}7H_2O$, 9 μM $MnSO_4{\cdot}7H_2O$, 45 μM H_3BO_4, 3 μM $ZnSO_4{\cdot}7H_2O$, 0.2 μM $CuSO_4{\cdot}7H_2O$, 0.05 μM $Na_2MoO_4{\cdot}2H_2O$. Whole roots were harvested 0, 1, 3 and 6 h after supplementation with $(NH_4)_2SO_4$.

To measure plant growth and ammonium contents, germinated seeds were cultured for 4 d in modified half-strength Kimura B (KB) solutions containing NH_4^+ or NO_3^- as the sole N source. The original half-strength KB nutrient solution contained macronutrients [0.18 mM $(NH_4)_2SO_4$, 0.27 mM $MgSO_4{\cdot}7H_2O$, 0.09 mM KNO_3, 0.18 mM $CaNO_3{\cdot}4H_2O$ and 0.09 mM KH_2PO_4] and micronutrients [20 μM Na_2EDTA-Fe(II)$\cdot 3H_2O$, 9.0 μM $MnCl_2{\cdot}4H_2O$, 46 μM H_3BO_3, 9.0 μM $Na_2MoO_4{\cdot}4H_2O$, 0.7 μM $ZnSO_4{\cdot}7H_2O$ and 0.3 μM $CuSO_4{\cdot}5H_2O$] at pH 5.8. For the modified KB nutrient, 0.18 mM $(NH_4)_2SO_4$ and 0.09 mM KNO_3 were replaced with appropriate concentrations of $(NH_4)_2SO_4$ or KNO_3, and 0.18 mM $CaNO_3{\cdot}4H_2O$ was replaced with 0.18 mM $CaCl_2$. Detailed information on the constituents of solutions is given in Supplementary data Table S1.

To analyse the effects of MSX on *cipk9* phenotypes, germinated seeds were cultured for 4 d in modified half-strength KB solutions containing an N source and MSX as follows: Solution 1, both NH_4^+ and NO_3^-; Solution 2, 0.5 mM $(NH_4)_2SO_4$; Solution 3, 0.5 mM KNO_3; Solution 4, 1 μM MSX; and Solution 5, 0.5 mM $(NH_4)_2SO_4$ and 1 μM MSX. Detailed information on the constituents of solutions is given in Supplementary data Table S2.

To examine the effect of potassium ions (K^+) on *cipk9* and *idd10* phenotypes, germinated seeds were cultured in modified half-strength KB solutions containing K^+ and NH_4^+ as follows: Solution A, 10 mM K^+ and no NH_4^+; Solution B, 10 mM K^+ and 0.5 mM NH_4^+; Solution C, no K^+ and 0.5 mM NH_4^+; and Solution D, no K^+ and no NH_4^+. Detailed information on the constituents of solutions is given in Supplementary data Table S3.

To test N-dependent root growth and chlorophyll biosynthesis, 0.1, 0.25, 0.5 and 1 mM NO_3^- or NH_4^+ were added to the N-free nutrient solution (Supplementary data Table S1). Primary root length was measured after 4 d of growth. The NH_4^+ content was also measured in roots from 4-day-old plants grown in a solution containing 0.5 mM NO_3^- or $(NH_4)_2SO_4$. Detailed information on the constituents of solutions is given in Supplementary data Table S1.

CIPK lines containing T-DNA insertions were identified using the RiceGE database (http://signal.salk.edu/cgi-bin/RiceGE); *cipk8* (PFG_1C-09231.R), *cipk14* (PFG_1A-20931.L) and *cipk23* (PFG_3D-01239.L) were identified in this way. In addition, *cipk9* was isolated from the *Ds*-tagging mutant pool (Chin *et al.*, 1999).

RNA extraction and qRT–PCR analysis

Total cellular RNA was isolated using the RNeasy Plant Mini Kit (Qiagen, Valencia, CA, USA) and treated with RQ-RNase free DNase (Promega, Madison, WI, USA). A reverse transcriptase RNase H (Toyobo, http://www.toyobo-global.com/) transcription kit was used to synthesize cDNA according to the manufacturer's instructions (Promega). qRT–PCR products were quantified using Illumina Eco 3.0 software (Illumina, San Diego, CA, USA), and values were normalized against *UBIQUITIN*, *OsUBC3* (Yang *et al.*, 2017; Hsieh *et al.*, 2018), *UBQ1* (Wang *et al.*, 2018), *UBQ5* (Wu *et al.*, 2017) and 18S rRNA (Jain *et al.*, 2006; Ishikawa-Sakurai *et al.*, 2014) levels in the same samples. All primers used for qRT–PCR are presented in Supplementary data Table S4.

Chromatin immunoprecipitation assay

Samples of 8 g of calli from transgenic rice plants expressing *IDD10-GFP* were prepared for ChIP analysis.

Pre-absorption with a pre-immune serum was performed before immunoprecipitation with an anti-GFP (green fluorescent protein) monoclonal antibody (Clontech). Immunoprecipitates were analysed using qPCR. Each input DNA level was used as a control for normalizing the levels of immunoprecipitated DNA in the qPCR assay (Je *et al.*, 2010). All primers used for ChIP-PCR are listed in Supplementary data Table S5.

Electrophoretic mobility shift assay

N-terminal *IDD10* cDNA sequences (67–254 amino acids) were sub-cloned into the pGEX5×-1 expression vector to produce the *pGEX5×-1-IDD10* plasmid. *Escherichia coli* strain BL21 DE3 was transformed with *pGEX5×-1-IDD10* to enable production of IDD10 recombinant protein.

A single colony of BL21 *E. coli* harbouring *pGEX5×-1-IDD10* plasmid was inoculated into liquid LB medium containing ampicillin at 100 μg ml^{-1} and 0.5 mM isopropyl-β-D-thiogalactopyranoside (IPTG) was added when the optical density (OD) reached 0.2. After 4 h of induction at 28 °C, cells were harvested by centrifugation at 4000 rpm for 5 min at 4 °C. The supernatant was then removed and the cells were resuspended in 1× phosphate-buffered saline (PBS) solution, and were subsequently sonicated for 15 min (three times, 5 min each). After sonication, the cell lysate was centrifuged at 12 000 rpm for 20 min at 4 °C, and the supernatant was then reacted with glutathione *S*-transferase (GST) beads for purification (Xuan *et al.*, 2013). The purified GST–IDD10 protein was examined using SDS–PAGE (Supplementary data Fig. S1).

For EMSA, a standard binding reaction was performed in a total volume of 20 μL by incubating 1 μg of purified protein with 40 000 cpm of ^{32}P-labelled DNA probe and 1 μg of poly(dI–dC) in reaction buffer [25 mM HEPES-KOH, pH 7.5, 100 mM KCl, 0.1 mM EDTA, 10 % (v/v) glycerol, 1 mM dithiothreitol (DTT)] at room temperature for 30 min. The binding reaction products were resolved on an 8 % polyacrylamide gel run in 0.5× TBE buffer (Je *et al.*, 2010). For probe labelling, 30 nucleotide DNA fragments were synthesized and end-labelled with [γ-^{32}P]ATP using T4 polynucleotide kinase (NEB, Ipswich, MA, USA). The primers used to produce the EMSA probes are listed in Supplementary data Table S5.

Transcriptional activity analysis

Constructs containing an effector (*35S:IDD10*), reporters (P2, P3, mP2 and mP3) and an internal control (*35S:LUC*) were used to co-transform arabidopsis protoplasts (Yamaguchi *et al.*, 2010). To generate *p35S:IDD10*, the *GAL4BD* region of the *p35S:GAL4BD* vector was replaced by *IDD10* cDNA using the *Bam*HI and *Sac*I restriction sites. To obtain reporter vectors, 1.5 kb portions of the *CIPK9* or *CIPK14* promoter sequences were amplified using PCR. Expression of β-glucuronidase (GUS) was normalized against luciferase expression (Xuan *et al.*, 2013). Polyethylene glycol (PEG)-mediated transformation and activity assays were performed as described previously (Yoo *et al.*, 2007). The primers used to amplify the *CIPK9* and *CIPK14* promoter fragments are listed in Supplementary data Table S5.

Yeast one-hybrid analysis

The 1.5 kb regions from the *CIPK9* and *CIPK14* promoters were cloned into the *pHISi* vector, and the open reading frame (ORF) sequence of *IDD10* was cloned into the *pGAD424* vector. The appropriate *pCIPK-His* plasmid was transformed into yeast strain YM4271. Transformants containing each *CIPK* promoter were used as competent cells and transformed with *pGAD424-IDD10* or *pGAD424* empty vector. The growth of yeast cells on synthetic dropout media (-Leu and -Ura or -Leu and -Ura-His) was monitored.

Generation of transgenic plants

To generate plants overexpressing *AMT1;2* and *CIPK9*, the *AMT1;2* and *CIPK9* ORFs were cloned into the *Bam*HI and *Hin*dIII restriction sites of the *pGA1611* binary vector to produce *pGA1611-AMT1;2* and *pGA1611-CIPK9*, in which *AMT1;2* and *CIPK9* were expressed under the control of the *UBIQUITIN* promoter. Rice calli were transformed with *pGA1611-AMT1;2* and *pGA1611-CIPK9* via *Agrobacterium*-mediated transformation (Chin *et al.*, 1999).

Determination of ammonium content

Enzymatic determination of NH_4^+ content in roots was performed using the F-kit (Roche), according to the manufacturer's instructions (Oliveira *et al.*, 2002).

GUS assay

Seven-day-old seedlings of *CIPK9::Ds* (*cipk9* heterozygotes) were collected in 15 mL Falcon tubes containing GUS staining solution. All tubes were wrapped in foil and kept at 37 °C for 2 d (Chin *et al.*, 1999).

Localization of CIPK9 *in plants*

The *CIPK9* ORF was cloned into the *pABindGFP* destination plasmid (Bleckmann *et al.*, 2010) to produce *CIPK9:GFP*, in which the *CIPK9* ORF, fused to the *GFP* sequence at the N-terminus, was expressed under the control of the 35S promoter. This vector was expressed in *Nicotiana benthamiana* leaves via *Agrobacterium*-mediated transient expression (Kim *et al.*, 2009). GFP fluorescence was detected using an Olympus confocal laser scanning microscope (Fluoview FV 1000, http://www.olympus-global.com/).

Tissue culture regeneration

To produce plantlets from calli, four different tissue culture media (NB, N6-7-CH, N6S3-CH-I and N6S3-CH-II) were used. The regeneration methodology was as described previously (Kim *et al.*, 2004).

Southern blot analysis

Samples of 5 µg of genomic DNA were digested with *Eco*RI restriction endonucleases and separated on a 0.8 % agarose gel, followed by transfer to a nylon membrane. The blots were hybridized to probes in hybridization buffer containing 6× SSC, 5× Denhardt's, 0.5 % SDS, 50 nM Tris (pH 8.0), 10 nM EDTA, 0.1 mg mL^{-1} heat-denatured salmon sperm DNA and 5 % dextran sulphate. Final washes of the filters were carried out in 0.2× SSC and 0.1 % SDS for 15 min at 65 °C. The membranes were exposed to X-rays.

^{15}N uptake analysis

For hydroponic culture, rice seeds were surface-sterilized using 0.1 % Previcur N (Bayer, Monheim, Germany) for 15 min and germinated on paper towels at 37 °C for 3 d. Seedlings were transferred to, and pre-cultured in, deionized water for 2 weeks, and then grown in an N-free nutrient solution (Sonoda *et al.*, 2003) for 3 d before $^{15}NH_4^+$ uptake analysis. Plants were grown in a climate-controlled chamber under a 14 h/37 °C and 10 h/30 °C day–night cycle at 60 % relative humidity.

Roots were washed in 1 mM $CaSO_4$ for 1 min, and incubated for 6 min in N-free nutrient solution (pH 5.8) containing 200 µM $^{15}NH_4^+$ (95 atom % ^{15}N) as the sole N source. Roots were rinsed in 1 mM $CaSO_4$ for 1 min before harvest to remove the tracer from the apoplast. Freeze-dried 1.5 mg samples were subjected to ^{15}N analysis using isotope ratio mass spectrometry (DELTAplus XP, Thermo-Finnigan).

Statistical analyses

Statistical calculations were performed using Prism 5 (GraphPad, San Diego, CA, USA). Comparisons between groups were made using one-way analysis of variance (ANOVA; Brady *et al.*, 2015), followed by Bonferroni's correction for multiple comparisons. Differences in P-values < 0.05 were considered statistically significant. All data are expressed as the mean ± s.e.

RESULTS

Overexpression of AMT1;2 *does not rescue* idd10 *root growth inhibition*

IDD10 directly activates expression of *AMT1;2,* and NH_4^+ accumulates to lower cellular levels in *idd10* mutants than in wild-type plants (Xuan *et al.*, 2013). To investigate whether limited NH_4^+ uptake or low levels of cellular NH_4^+ were responsible for growth retardation of *idd10* roots, several lines overexpressing *AMT1;2* (*AMT1;2 OX*) were generated and crossed with *idd10* mutants. Analysis by qRT–PCR showed that *AMT1;2* levels in the roots of plants from the overexpression lines (*#1*, *#2*, *#4* and *#5*) were >20-fold higher than in wild-type roots (Fig. 1A). Line *AMT1;2 OX4*, which showed the highest expression of *AMT1;2* mRNA, was selected for crossing with *idd10* to examine the effect of combining the *idd10* mutation with *AMT1;2* overexpression.

The four genotypes (wild type, *idd10*, *AMT1;2 OX4* and *idd10/AMT1;2 OX4*) produced by crosses between *AMT1;2 OX4* and *idd10* lines were analysed using qRT–PCR to determine expression of *AMT1;2* and *IDD10* in 7-day-old roots (Supplementary data Fig. S2). Roots of *idd10/AMT1;2 OX4* and *AMT1;2 OX4* plants expressed similar levels of *AMT1;2* mRNA; however, *IDD10* expression was completely inhibited in both *idd10/AMT1;2 OX4* and *idd10* roots.

The growth responses of wild-type seedlings to nutrient solutions containing different concentrations (0.1, 0.25, 0.5 and 1 mM) of NO_3^- or NH_4^+ were determined. Concentrations of 1 mM NO_3^- or NH_4^+ produced the highest chlorophyll contents in leaves (Supplementary data Fig. S3A). Primary roots grown in NO_3^- were longer than primary roots grown in the same concentrations of NH_4^+ (Supplementary data Fig. S3B).

To evaluate the effect of *AMT1;2* overexpression on *idd10* root growth, wild-type, *idd10*, *idd10/AMT1;2 OX4* and *AMT1;2 OX4* roots were grown in nutrient solutions containing 1 mM NO_3^- or NH_4^+. Nitrogen-dependent root growth was measured in 7-day-old roots after incubation in the nutrient solutions for 4 d (Fig. 1B, C). A nutrient solution containing 1 mM KNO_3 produced no differences in primary root growth between wild-type, *idd10*, *idd10/AMT1;2 OX4* and *AMT1;2 OX* lines. Following 4 d of growth in a solution containing 1 mM NH_4^+, primary root lengths of *idd10/AMT1;2 OX4* and *idd10* were similar, and shorter than roots of wild-type and *AMT1;2 OX4* seedlings. The growth of wild-type and *AMT1;2 OX4* primary roots was similar in the solution containing 1 mM NH_4^+.

Cellular NH_4^+ content was determined in the roots of all four genotypes (Fig. 1D). Ammonium content was lowest in *idd10* roots, but accumulated to a similar level in *idd10/AMT1;2 OX4* and *AMT1;2 OX4* roots; this level was higher than that found in wild-type roots. These results suggest that enhancing NH_4^+ uptake and cellular NH_4^+ levels does not rescue the growth defect of *idd10* roots.

Expression of CIPK *genes is sensitive to ammonium*

To determine the genetic factors responsible for the defective root growth of *idd10*, NH_4^+-responsive regulatory genes, identified in an earlier analysis of transcriptomic data (Xuan *et al.*, 2013), were inspected. The expression of 12 *CIPK* genes out of a 31 member family in rice was noted to be sensitive to NH_4^+. To analyse *CIPK* gene expression in response to NH_4^+ further, 17-day-old wild-type plants grown without N were treated with 0.5 mM $(NH_4)_2SO_4$ for 0, 1, 3 and 6 h (Fig. 2A) and RNA was extracted from samples of whole roots. Expression of the 12 *CIPK* genes (*CIPK3*, *5*, *8*, *9*, *10*, *11*, *12*, *14/15*, *23*, *24* and *31*) was analysed using qRT–PCR to determine their responses to NH_4^+; *CIPK* expression was normalized against expression of the internal control genes *UBIQUITIN* (Fig. 2B), *OsUBC3*, *UBQ1*, *UBQ5* and 18S rRNA (Supplementary data Fig. S4A–D, respectively). Induction of *CIPK14* and *15* had to be calculated together

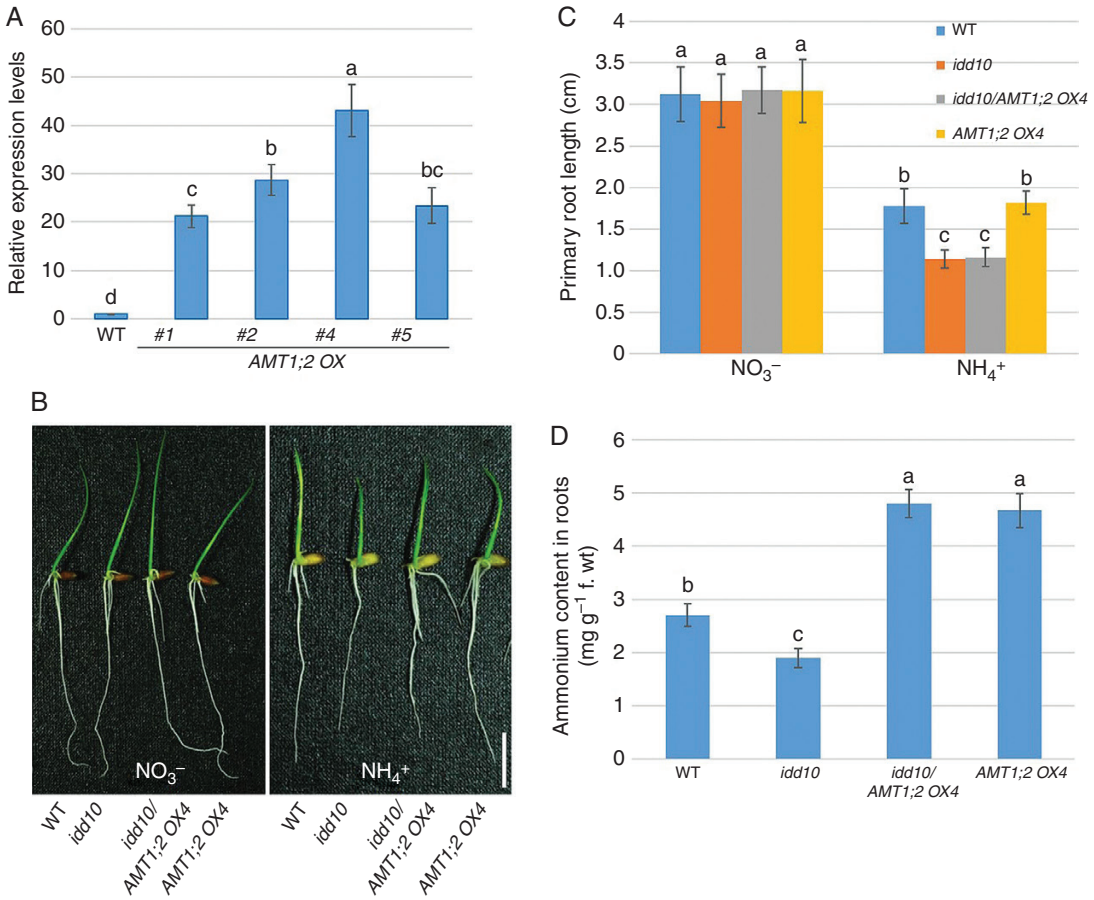

FIG. 1. Root growth and cellular NH_4^+ content of wild-type, *AMT1;2 OX*, *idd10* and *idd10/AMT1;2 OX4* plants. (A) *AMT1;2* expression levels in the wild type (WT) and four *AMT1;2* overexpression lines (*AMT1;2 OX*; *#1*, *#2*, *#4* AND *#5*) were monitored using QRT–PCR. *AMT1;2* MRNA levels in the samples were normalized against expression of *UBIQUITIN*. Data are means ± S.E. ($N = 3$). (B) Wild-type, *idd10*, *idd10/AMT1;2 OX4* and *AMT1;2 OX4* were grown for 4 d in half-strength KB nutrient solution containing either NO_3^- or NH_4^+ as the sole N source. Scale bar = 1 cm. (C) Primary root length measurements of the plants shown in (B). Data are means ± s.e. ($n > 10$ plants per line). (D) Cellular NH_4^+ levels in wild-type and mutant roots grown for 4 d in a nutrient solution containing NH_4^+ as the sole N source. Details of all nutrient media are in Supplementary data Table S1. Data are means ± s.e. ($n > 10$ plants per line); different letters indicate significant differences between results ($P < 0.05$).

as *CIPK14/15* due to extremely high homology (96 % identity) between their nucleotide sequences (Kurusu *et al.*, 2010).

Ammonium repressed expression of *CIPK3* in roots but induced expression of *CIPK5*, *CIPK8*, *CIPK9*, *CIPK10*, *CIPK14/15*, *CIPK23* and *CIPK31*; transcript levels of *CIPK11*, *CIPK12* and *CIPK24* were not altered by NH_4^+. *CIPK8*, *CIPK9* and *CIPK23* were induced >2-fold, while *CIPK14/15* showed a >10-fold increase (Fig. 2B).

In addition, NH_4^+-dependent expression of *CBL* genes was analysed (Supplementary data Fig. S5). Of the ten *CBL* genes, *CBL1*, *CBL2*, *CBL3* and *CBL6* were consistently induced by NH_4^+ supplementation; expression of *CBL2* and *CBL3* increased >2-fold. Expression of the other *CBL* genes was not altered by NH_4^+.

Five CIPK *genes are positively regulated by* IDD10 *in an* NH_4^+*-dependent manner*

To examine whether *IDD10* was involved in NH_4^+-responsive *CIPK* expression, the expression levels of the five *CIPK* genes (*CIPK8*, *CIPK9*, *CIPK14/15* and *CIPK23*) that were induced >2-fold by NH_4^+ treatment were examined in the roots of *idd10* and *IDD10 OX* (*OX2*) plants and their wild-type siblings. Seventeen-day-old wild-type seedlings were treated with 0.5 mM $(NH_4)_2SO_4$ for 0, 1, 3 and 6 h. Expression levels of the five genes were determined using qRT–PCR; *UBIQUITIN* (Fig. 3) and *OsUBC3* (Supplementary data Fig. S6) were used as internal normalization controls.

There were no differences in expression levels of any of the five *CIPK* genes between *idd10* and its wild-type siblings (Fig. 3A, C, E, G) or between *OX2* and its wild-type siblings (Fig. 3B, D, F, H) before NH_4^+ treatment. After NH_4^+ treatment, lower levels of induction of *CIPK* genes were observed in *idd10* than in wild-type plants; in contrast, induction of *CIPK* genes was higher in *OX2* than in wild-type plants following treatment. These results suggest that *IDD10* exerts positive effects on NH_4^+-mediated induction of *CIPK8*, *CIPK9*, *CIPK14/15* and *CIPK23*.

CIPK9 *is a direct target of* IDD10 *and its mutation results in sensitivity to ammonium*

As *IDD10* influenced NH_4^+-mediated induction of five *CIPK* genes, the possibility that they were directly activated by *IDD10* was examined by analysing 1.5 kb of their promoter sequences.

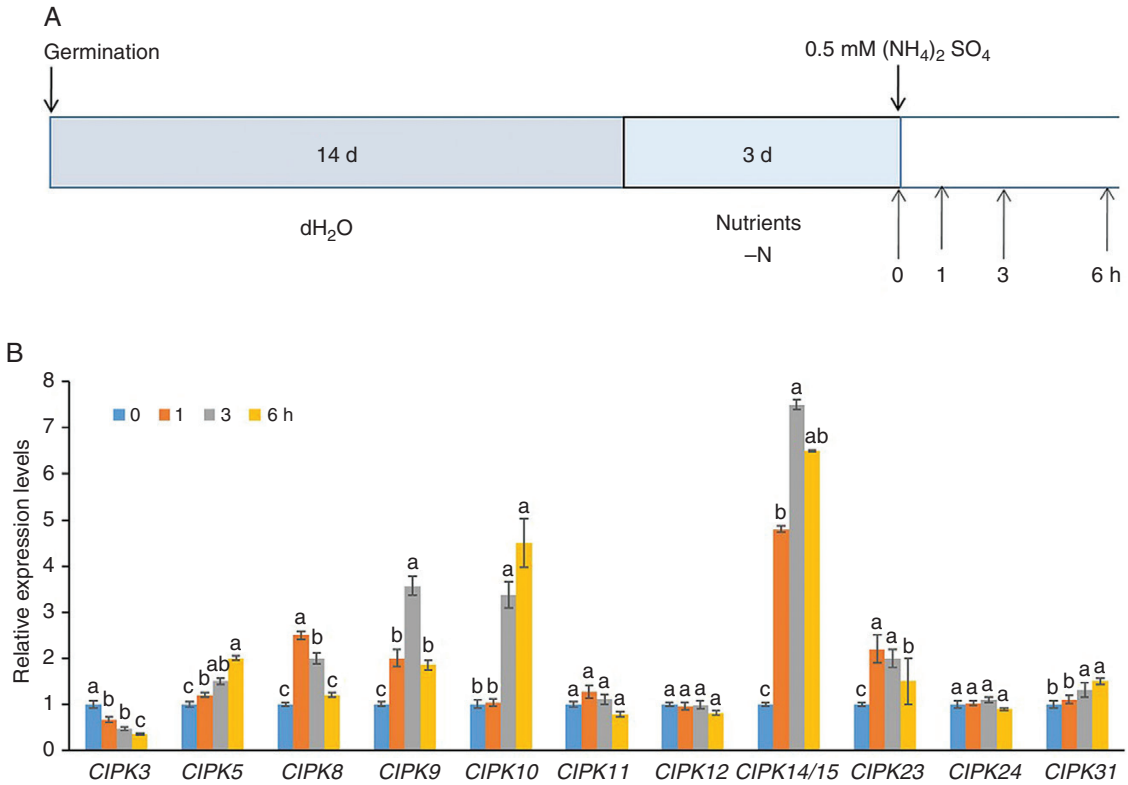

FIG. 2. Expression of *CIPK* genes in response to ammonium treatment. (A) Schematic showing NH_4^+ treatments and time points for sampling expression of NH_4^+-responsive *CIPK* genes. Wild-type seedlings were grown for 14 d in dH_2O, followed by 3 d in nutrient medium without N. The 17-day-old plants were then transferred to medium supplemented with 0.5 mM $(NH_4)_2SO_4$ for 0, 1, 3 and 6 h. Details of the nutrient medium are described in the Materials and Methods. (B) Responses of 12 *CIPK* genes (*CIPK3*, *5*, *8*, *9*, *10*, *11*, *12*, *14/15*, *23*, *24* and *31*) to NH_4^+ treatment. Expression levels of *CIPK* genes were determined using qRT–PCR. mRNA levels in the samples were normalized against those of *UBIQUITIN* mRNA. Data are means ± s.e. ($n = 3$); different letters indicate significant differences between results ($P < 0.05$).

The putative IDD10-binding motif ($TTTGTC^G/_C$) (Xuan *et al.*, 2013) was found in the *CIPK8*, *CIPK9* and *CIPK14* promoters, but not in the *CIPK15* and *CIPK23* promoters (Fig. 4A). The IDD family protein JKD activates the *SCR* and *MGP* promoters even though they lack the putative IDD-binding motif, suggesting that IDD proteins have diverse binding modes (Ogasawara *et al.*, 2011).

To determine whether *IDD10* binds directly to the *CIPK8*, *CIPK9*, *CIPK14*, *CIPK15* and *CIPK23* promoters, ChIP assays were performed using *IDD10-GFP* transgenic plants. Immunoprecipitates obtained from *IDD10-GFP* transgenic plants in the presence or absence of a GFP antibody were analysed using qRT–PCR. In total, 16 primer sets were used to amplify 16 promoter regions (P1–P16) from the five *CIPK* genes; these included four regions containing putative IDD10-binding motifs. All the promoter regions were located within 1.5 kb from the ATG start sites of the genes. qRT–PCR analysis detected significantly higher amounts of DNA from the P5 and P9 regions following immunoprecipitation with a GFP antibody compared with controls without the antibody (Fig. 4B). These two regions corresponded to the sections of the *CIPK9* and *CIPK14* promoters containing the putative IDD10-binding motifs.

A yeast one-hybrid assay was also used to confirm whether IDD10 activated the *CIPK* promoters. The 1.5 kb regions from the *CIPK8*, *CIPK9*, *CIPK14*, *CIPK15* and *CIPK23* promoters were examined for transcriptional activation in the yeast one-hybrid system. IDD10 was able to activate the *CIPK9* and *CIPK14* promoters in yeast (Supplementary data Fig. S7), consistent with the results obtained from the ChIP assays.

To verify that IDD10 activated *CIPK9* and *CIPK14* via IDD-binding motifs, EMSA and an *in vivo* transcription activation assay were performed. Mutant P5 and P9 (mP5 and mP9) regions were created by changing the binding motif sequence in P5 from TTTGTCG to TTTTTTT and the sequence in P9 from AAACAGG to AAAAAAA. EMSA was used to determine the binding affinities of IDD10 for the wild-type and mutated P5 and P9 regions. The assays showed that IDD10 bound to P5 and P9, but not to mP5 and mP9 (Fig. 5A, C).

To confirm that these *cis*-elements were responsible for transcriptional activation of the *CIPK9* and *CIPK14* promoters by IDD10 *in vivo*, transient expression assays were performed using an arabidopsis protoplast system (Fig. 5B, D). Protoplast cells were co-transformed with the *35S:IDD10* plasmid and a vector expressing GUS under the control of either the wild-type *CIPK9* (P5) and *CIPK14* (P9) promoters or promoters containing the mutated motifs (mP5 and mP9); *35S:LUC* was used as an internal control to normalize transformation efficiency in each assay. GUS activity was approx. 2-fold higher in protoplasts expressing *IDD10* under the P5 and P9 promoters than in protoplasts expressing the reporter alone or containing either mutated promoter. This indicates that IDD10 activates expression of *CIPK9* and *CIPK14* directly by binding to their promoters.

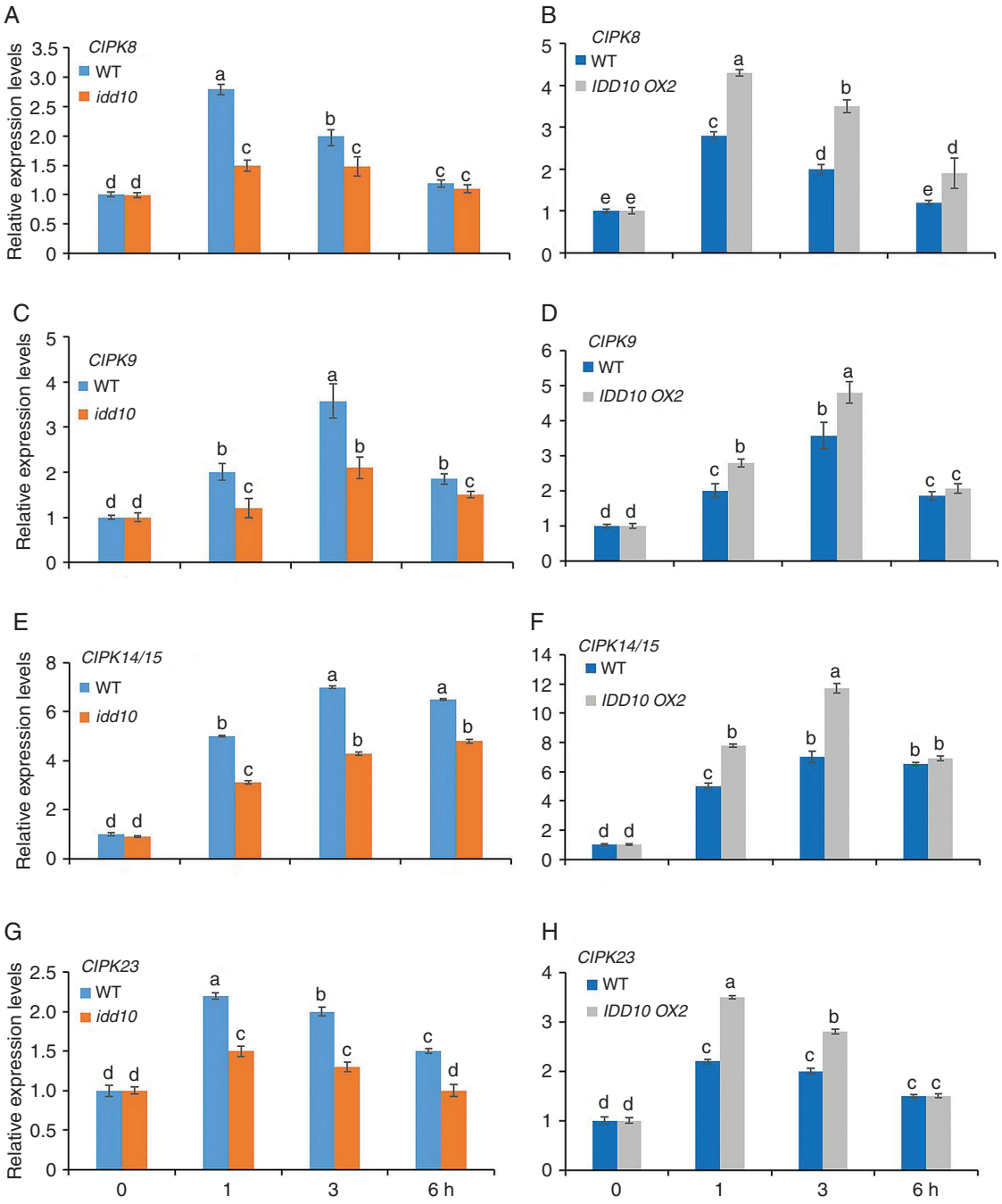

FIG. 3. Responses of five *CIPK* genes in roots of *idd10* and *IDD10 OX2* plants to exposure to NH_4^+. (A, C, E and G) Expression of *CIPK8*, *9*, *14/15* and *23* in *idd10* and wild-type plants. (B, D, F and H) Expression of *CIPK8*, *9*, *14/15* and *23* in *IDD10 OX2* and wild-type plants. Levels of *CIPK* mRNA expression were determined using qRT–PCR. Sample mRNA levels were normalized against those of *UBIQUITIN* mRNA. Seedling growth conditions and treatments were as shown in FIG. 2A; total roots were sampled 0, 1, 3 and 6 h after the addition of NH_4^+. Data are means ± s.e. ($n = 3$); different letters indicate significant differences between results ($P < 0.05$).

CIPK9 *and* CIPK23 *mutants show* NH_4^+*-sensitive phenotypes*

To determine whether *CIPK* mutants exhibited NH_4^+-sensitive root growth, *cipk8*, *cipk14* and *cipk23* T-DNA insertion mutants and a *cipk9 Ds* gene trap mutant (Chin *et al.*, 1999) were isolated as described in the Materials and Methods (Fig. 6A). Expression of each *CIPK* gene was examined in the roots of 7-day-old wild-type and *cipk* mutant seedlings (Supplementary data Fig. S8). Expression of *CIPK8*, *CIPK9* and *CIPK23* was completely suppressed in their respective mutants. A low level of *CIPK14* mRNA was detected in *cipk14* mutants; this may result from the high sequence homology between *CIPK14* and *CIPK15* (Kurusu *et al.*, 2010) (Supplementary data Fig. S8).

The primary root lengths of *cipk* mutants were determined following growth in nutrient solutions containing 1 mM NO_3^- or NH_4^+ (Fig. 6B, C). No significant differences between wild-type

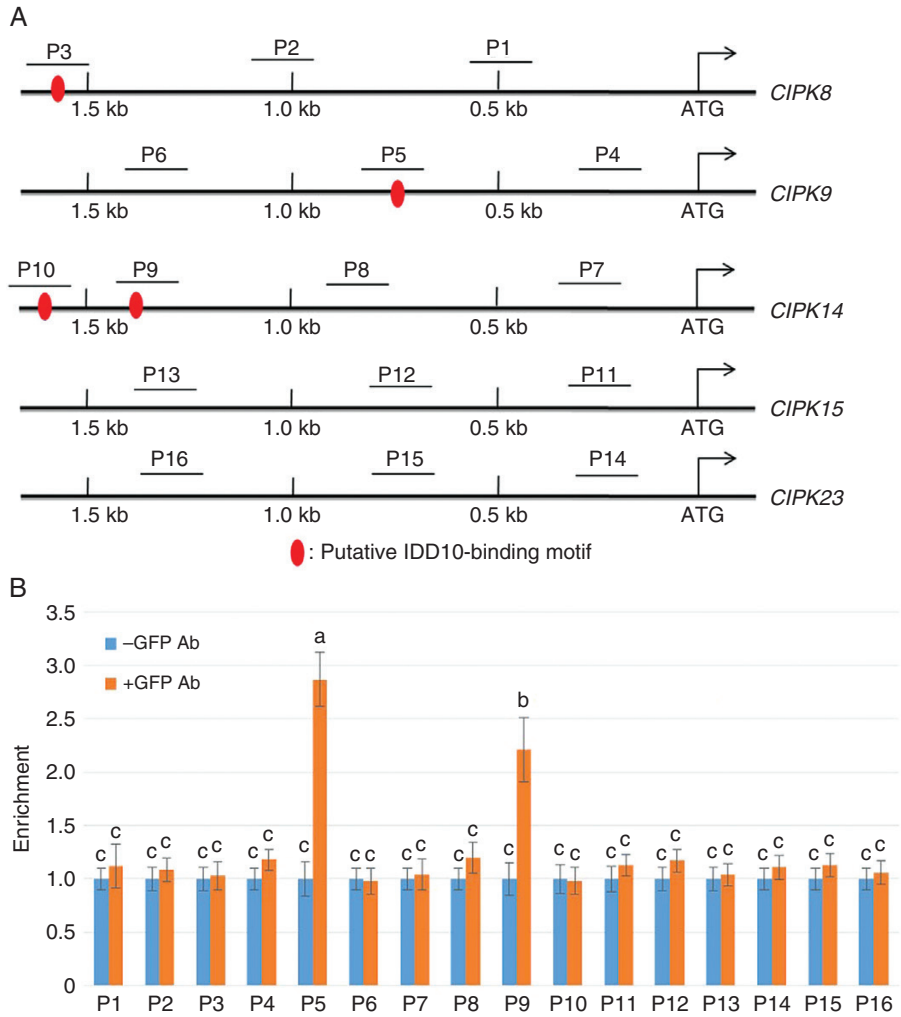

FIG. 4. Binding affinity of IDD10 for the promoters of *CIPK9* and *CIPK14*. (A) Schematic diagram showing the locations of putative IDD10-binding motifs in 1.5 kb regions of the promoters of five different *CIPK* genes. The areas amplified by the probes P1–P16 in the ChIP assay are underlined. (B) Results of the ChIP assay. DNA was immunoprecipitated and amplified to determine the extent to which IDD10 bound regions P1–P16 within a 1.5 kb portion of each *CIPK* promoter. The relative ratios of immunoprecipitated DNA to input DNA were determined using qPCR. Input DNA was used to normalize the data. DNA immunoprecipitated without addition of GFP antibody (Ab) was used as a control. Data are means ± s.e. ($n = 3$); different letters indicate significant differences between results ($P < 0.05$).

and *cipk* mutants were observed after growth in NO_3^- solution. In contrast, the primary roots of *cipk9* and *cipk23* were significantly shorter than wild-type roots after 4 d of growth in NH_4^+ solution. Cellular NH_4^+ content was measured in roots of 4-day-old wild-type, *cipk8*, *9*, *14* and *23* plants grown in nutrient solution containing NH_4^+ (Fig. 6D). *cipk9* and *cipk23* plants contained lower levels of cellular NH_4^+ than wild-type plants, but the NH_4^+ content of *cipk8* and *cipk14* was similar to that of wild-type roots. Together, these results show that *CIPK9* and *CIPK23* exhibit NH_4^+-sensitive phenotypes.

Comparative analysis of NH_4^+-sensitive root growth in cipk9 *and* idd10

Although it is likely that *IDD10* influences the effect of NH_4^+ on the expression and phenotypes of both *CIPK9* and *CIPK23*, only *CIPK9* was found to be a direct target of IDD10. The expression pattern of *CIPK9* was therefore analysed in greater detail to compare its effect on NH_4^+-dependent root phenotypes with that of *IDD10*.

The pattern of *CIPK9* expression was examined by a qRT–PCR analysis of different tissues from wild-type plants and by GUS staining the *cipk9::Ds* insertion mutant (Chin *et al.*, 1999) *in planta* (Supplementary data Fig. S9). Both analyses showed that *CIPK9* was expressed in all tissues. To determine the subcellular localization of *CIPK9*, CIPK9–GFP was transiently expressed in *N. benthamiana* leaves using *Agrobacterium*-mediated transformation. Strong GFP signals were detected in both the nuclei and cytosol (Fig. 7B).

To analyse the hypersensitivity of root growth of *cipk9* mutants to NH_4^+ further, *CIPK9* revertants (Rev.) and overexpression lines (*OX*) were generated. Six revertants were obtained from *cipk9* seeds via tissue culture regeneration (Fig. 7A). Southern blot hybridization and sequencing analysis of revertants confirmed excision of the *Ds* element from its original

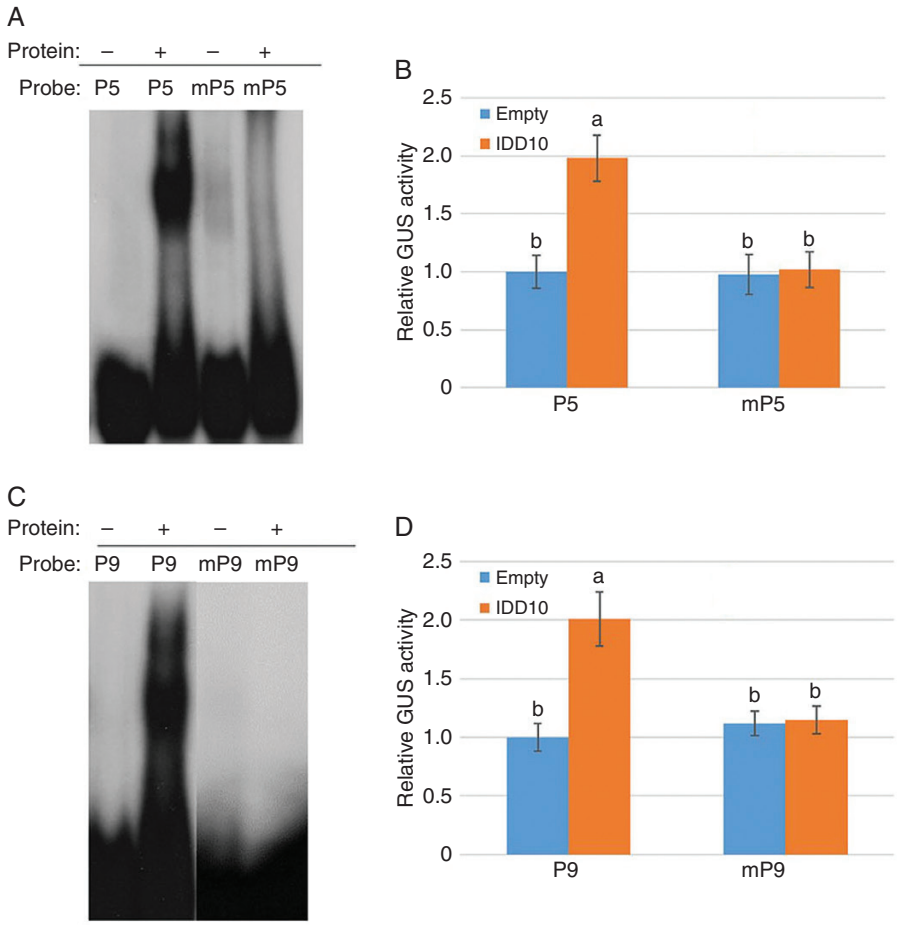

FIG. 5. Activation of *CIPK9* and *CIPK14* mediated by binding of IDD10 to IDD-binding motifs. (A) Binding affinities of IDD10 for the native IDD10-binding motif (TTTGTCG; P5) from the *CIPK9* promoter and a mutated motif (TTTTTTT; mP5). (B) Activation of the native *CIPK9* promoter (P5) and the mutated promoter (mP5) in protoplasts co-transfected with IDD10. (C) Binding affinities of IDD10 for the native IDD10-binding motif (AAACAGG; P9) from the *CIPK14* promoter and a mutated motif (AAAAAAA; mP9). (D) Activation of the native *CIPK14* promoter (P9) and the mutated promoter (mP9) in protoplasts co-transfected with IDD10. Binding affinities (A and C) of IDD10 for native (P5 and P9) and mutated (mP5 and mP9) putative IDD10-binding motifs were determined using EMSA. Transient expression assays (B and D) were performed in arabidopsis protoplasts co-transfected with IDD10 and vectors expressing GUS under the control of a 1.5 kb promoter from *CIPK9* (B) or *CIPK14* (D) containing either native or mutated IDD-binding motif sequences; co-transfection with empty vector was used as a control. Luciferase expression driven by the 35S promoter was used as an internal control for normalizing GUS expression data. Data in (B) and (D) are means ± s.e. ($n = 3$); different letters indicate significant differences between results ($P < 0.05$).

insertion site in the *CIPK9* locus (Supplementary data Fig. S10). In the overexpression lines, *CIPK9* cDNA was expressed under the control of the *UBIQUITIN* promoter.

Root growth, ammonium content and NH_4^+ uptake in *CIPK9* Rev., *CIPK9 OX*, *cipk9*, *idd10* and wild-type plants were measured and compared. No notable differences in root growth were observed between these five lines during culture in nutrient solution with NO_3^- as the sole N source (Fig. 7C, D). When NH_4^+ was the sole N source, the primary root length of Rev. plants resembled that of wild-type and *OX* plants; in contrast, the primary roots of *cipk9* and *idd10* mutants, although similar in length to each other, were shorter than those of the other genotypes (Fig. 7C, D). The internal NH_4^+ content of seedlings grown in nutrient solution containing NH_4^+ was measured and compared (Fig. 7E). The levels of NH_4^+ that accumulated in the roots of *cipk9* and *idd10* mutants were similar, and lower than levels in the other genotypes. There were no significant differences between NH_4^+ levels in wild-type, Rev. and *CIPK9 OX* seedlings. To determine whether *CIPK9* affected NH_4^+ uptake, short-term influx of ^{15}N-labelled ammonium into roots of 17-day-old wild-type, *idd10*, *cipk9*, Rev. and *CIPK9 OX* plants was measured (Fig. 7F). Roots were exposed to 200 μM $^{15}NH_4^+$ for 6 min; the ^{15}N influx was measured as μmol g^{-1} root d. wt h^{-1} (Yuan *et al.*, 2007, 2013). ^{15}N-labelled ammonium influx into *cipk9* and *idd10* mutants was similar and lower than influx into wild-type, Rev. and *CIPK9 OX* roots. Influx into *CIPK9 OX* roots was slightly lower than that into wild-type or Rev. roots.

As *idd10* and *cipk9* mutants exhibited the same root phenotypes, the possibility that expression of *AMT1;2* was altered in *cipk9* mutants was examined (Supplementary data Fig. S11). qRT–PCR was performed to measure expression of *AMT1;2* mRNA in wild-type, *idd10*, *cipk9*, Rev. and *OX* plants. Similar levels of *AMT1;2* mRNA were observed in *cipk9* and *CIPK9 OX* seedlings, indicating that *CIPK9* did not affect steady-state levels of *AMT1;2* mRNA.

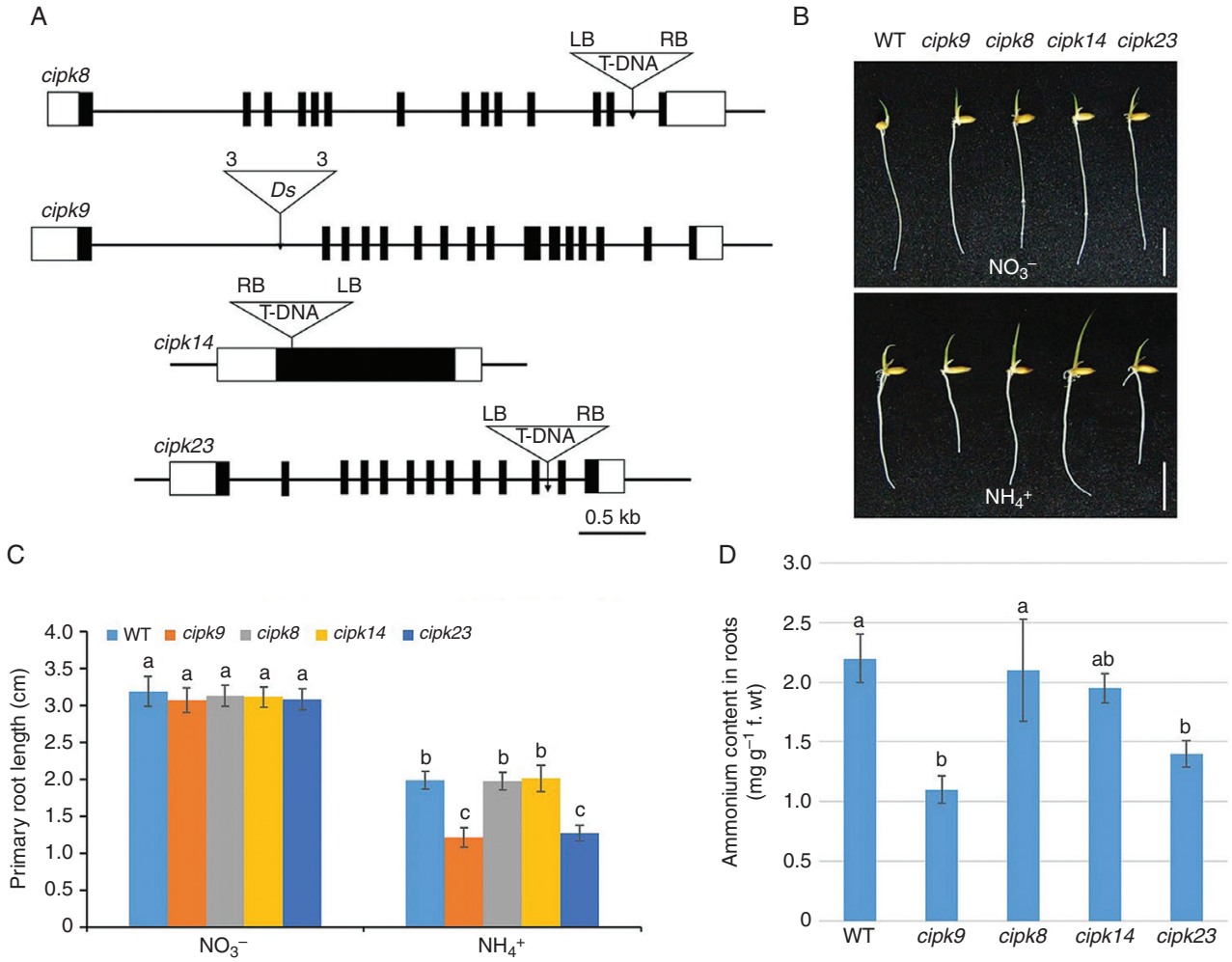

FIG. 6. Gene structure, root growth and cellular NH_4^+ content of *CIPK* mutants. (A) Schematic diagrams showing gene structures of the *CIPK* insertion mutants, *cipk8*, *cipk9*, *cipk14* AND *cipk23*. Black boxes, exons; white boxes, untranslated regions. Triangles indicate T-DNA or *Ds* insertion sites; '3' and '5' indicate the 3' and 5' ends of *Ds*, respectively; RB, right border of T-DNA; LB, left border of T-DNA. Scale bar = 0.5 kb. (B) Appearances of wild-type (WT), *cipk8*, *cipk9, cipk14* and *cipk23* seedlings after 4 d growth in nutrient solution containing either NO_3^- or NH_4^+ as the sole N source (Supplementary data Table S1). Scale bar = 1 cm. (C) Primary root lengths of wild-type, *cipk8*, *cipk9*, *cipk14* and *cipk23* seedlings grown as in (B). (D) Cellular NH_4^+ levels in roots of each line after 4 d growth in nutrient solution containing NH_4^+ as the sole N source. Data in (C) and (D) are means ± s.e. ($n > 10$ plants per line); different letters indicate significant differences between results ($P < 0.05$).

Overall, *cipk9* and *idd10* mutants showed an extremely similar pattern of sensitivity to NH_4^+, as measured by growth rate, cellular NH_4^+ level and NH_4^+ uptake in roots. It is therefore likely that *IDD10* and its target gene *CIPK9* are involved in the same signalling pathway mediating root growth in response to NH_4^+.

Overexpression of CIPK9 *rescues* NH_4^+*-sensitive root growth in* idd10

To understand the genetic relationship between *IDD10* and *CIPK9*, *CIPK9 OX* plants were crossed with *idd10* mutants. Ammonium-responsive root growth and cellular NH_4^+ content were examined in wild-type, *idd10*, *CIPK9 OX* and *idd10/CIPK9 OX* plants segregating from the same cross. A qRT–PCR analysis showed that levels of *CIPK9* mRNA were approximately ten times higher in *idd10/CIPK9 OX* and *CIPK9 OX* roots than in wild-type and *idd10* roots (Fig. 8A). No significant differences in root length between genotypes were observed when plants were grown in nutrient solution containing NO_3^- (Fig. 8B, C). When grown in nutrient solution containing NH_4^+, however, *idd10/CIPK9 OX* produced longer roots than *idd10* plants, while wild-type, *idd10/CIPK9 OX* and *CIPK9 OX* plants exhibited primary roots of similar lengths (Fig. 8B, C). The cellular NH_4^+ content was measured in roots of 7-day-old seedlings grown for 4 d in nutrient solution containing NH_4^+ (Fig. 8D). Seedlings with the *idd10/CIPK9 OX* genotype accumulated a higher level of cellular NH_4^+ than did *idd10* seedlings. Wild-type, *idd10/CIPK9 OX* and *CIPK9 OX* seedlings all contained similar amounts of cellular NH_4^+. These data strongly suggest that *CIPK9* acts downstream of *IDD10* in the signalling pathway mediating NH_4^+-sensitive root growth.

DISCUSSION

Exposure to high concentrations of exogenous NH_4^+ inhibits the elongation of primary roots in rice (Hirano *et al.*, 2008;

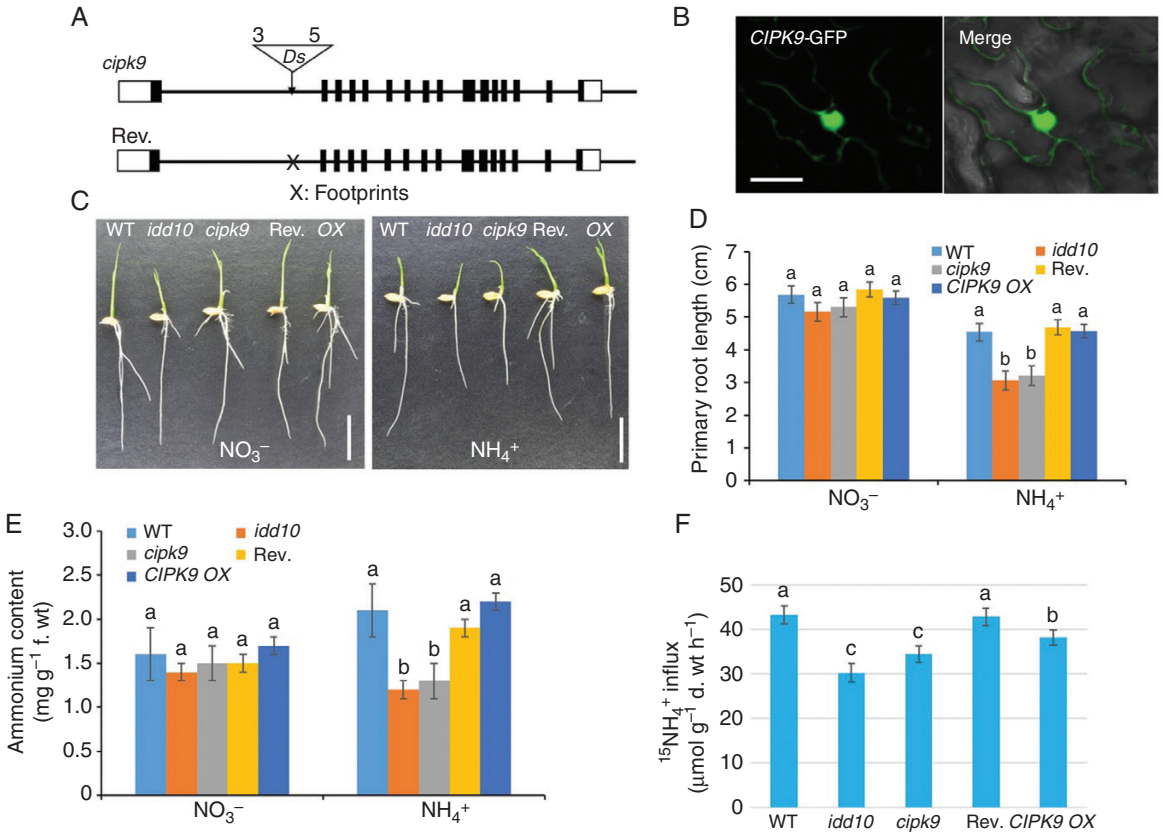

FIG. 7. Gene structures of *CIPK9* and its revertant, sub-cellular localization of CIPK9, and N-responsive root growth, NH_4^+ content and $^{15}NH_4^+$ uptake in *CIPK9* and *IDD10* mutants. (A) Schematic diagrams showing the genomic structures of the *CIPK9*::*Ds* insertion mutant and its revertant. Black boxes, exons; white boxes, untranslated regions. The triangle indicates the *Ds* insertion site; '3' and '5' indicate the 3′ and 5′ ends of *Ds*, respectively. *Ds* was excised from revertant plants leaving a footprint 'X' in the first intron. (B) Transient expression of CIPK9–GFP in *Nicotiana benthamiana* leaves. Left panel, confocal microscopy of green fluorescent protein (GFP); right panel, overlay of light microscopy image with GFP signal from the same tissue. Scale bars = 20 μm. (C) Appearance of wild-type (WT), *idd10*, *cipk9*, *CIPK9* revertant (Rev.) and *CIPK9* overexpressing (*OX*) seedlings after 4 d growth in nutrient solutions with either NO_3^- or NH_4^+ as the sole N source (Supplementary data Table S1). Scale bar = 1 cm. (D) Measurements of primary root lengths of plants grown as shown in (C) ($n > 10$ plants per line). (E) Endogenous NH_4^+ levels in roots of seedlings grown for 4 d in a nutrient solution with either NO_3^- or NH_4^+ as the sole N source ($n > 10$ plants per line). (F) Analysis of $^{15}NH_4^+$ influx into roots of wild-type, *idd10*, *cipk9*, Rev. and *CIPK9 OX* plants. Ammonium uptake into rice roots was determined following exposure to 200 μM ^{15}N-labelled NH_4^+. Data shown in (D) and (E) are means ± s.e.; data shown in (F) are means ± s.d. ($n > 10$ plants per line). In all cases, different letters indicate significant differences between results ($P < 0.05$).

Shimizu *et al.*, 2009). Root elongation of *idd10* mutants is inhibited, however, even at NH_4^+ levels that are optimal for growth of normal rice seedlings (Xuan *et al.*, 2013). The molecular mechanisms underlying the hypersensitivity to NH_4^+ of root growth in *idd10* mutants were therefore explored.

The hypothesis that root growth retardation of *idd10* resulted from limited intracellular NH_4^+ was tested first. This hypothesis was formed from the following observations: first, that *IDD10* regulates the expression of N uptake genes; secondly, that *idd10* plants contain low levels of intracellular NH_4^+; and, finally, that treatment with the glutamine synthetase inhibitor MSX, which suppresses NH_4^+-mediated inhibition of root growth, leads to an increase in intracellular levels of NH_4^+ in both wild-type and *idd10* plants (Hirano *et al.*, 2008; Shimizu *et al.*, 2009; Xuan *et al.*, 2013). Our results demonstrated, however, that the level of internal NH_4^+ was not related to the NH_4^+-dependent growth defect in *idd10* roots.

This prompted us to examine regulatory factors whose expression was influenced by both NH_4^+ and *IDD10*. A second hypothesis was proposed that growth retardation in *idd10* mutants resulted from disruption of the signalling mechanisms underlying NH_4^+ tolerance. CIPK proteins regulate potassium, NH_4^+ and NO_3^- uptake and signalling in plants (Xu *et al.*, 2006; Pandey *et al.*, 2007; Ho *et al.*, 2009; Hu *et al.*, 2009; Liu *et al.*, 2012; Li *et al.*, 2014; Straub *et al.*, 2017). We showed that five *CIPK* genes and four *CBL* genes were induced by NH_4^+, with two genes (*CIPK9* and *CIPK14*) being directly regulated by *IDD10*. Ammonium-mediated expression levels of *CIPK15* and *CIPK23* varied with expression of *IDD10* even though no putative IDD10-binding motifs were detected in their promoters. Moreover, the roots of *cipk9* and *cipk23* seedlings showed NH_4^+-sensitive phenotypes, as both mutants had short roots that accumulated low cellular NH_4^+ (Fig. 6). These data strongly imply that the CBL–CIPK cassette plays a role in NH_4^+ signalling, that *IDD10* directly regulates the expression of some *CIPK* genes, and that *IDD10* and *CIPK* genes interact to regulate NH_4^+ signalling.

The most notable finding was that disrupting *CIPK9*, a direct target of *IDD10*, produced almost identical root phenotypes to disruption of *IDD10*. Moreover, roots of *cipk9* and *idd10*

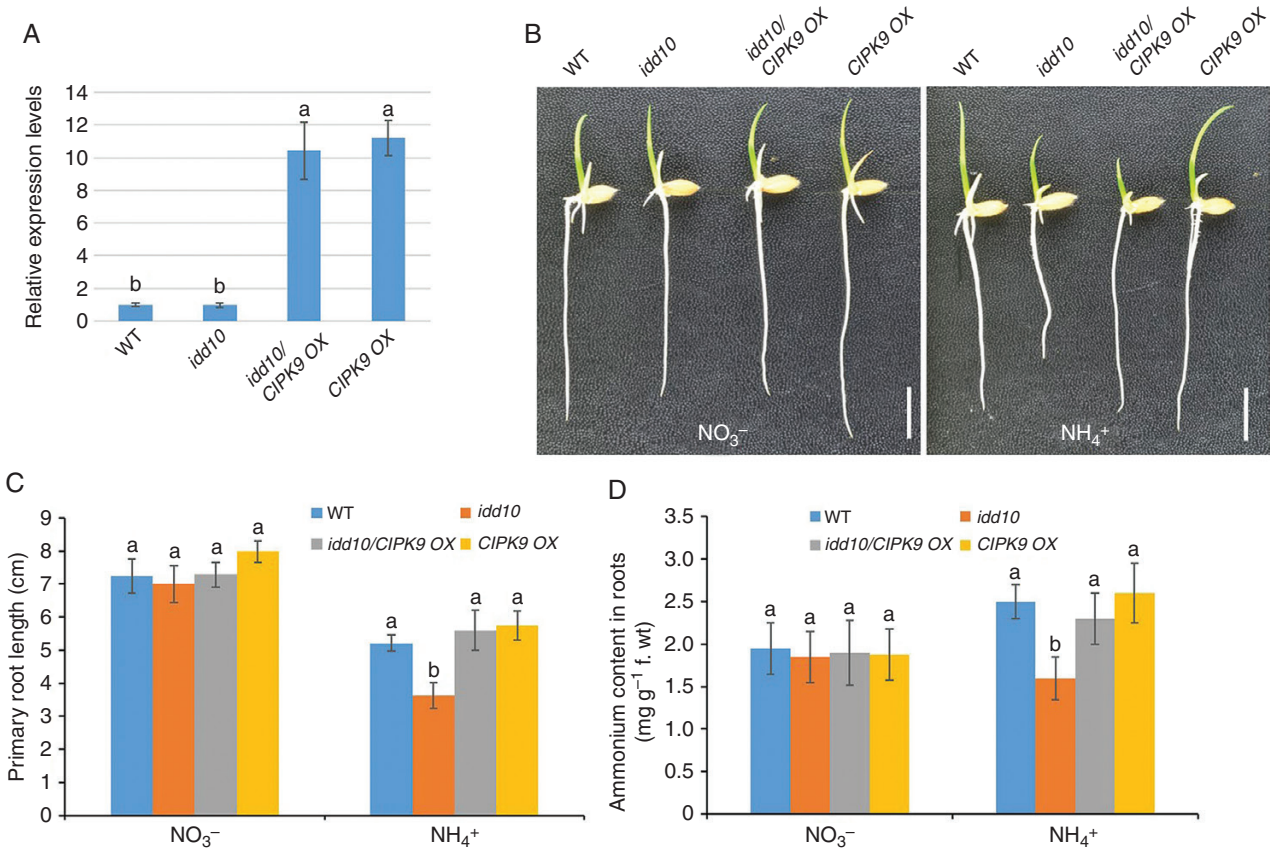

FIG. 8. *CIPK9* expression, primary root growth and cellular NH_4^+ levels in plants produced by crosses between *IDD10* and *CIPK9 OX*. (A) Levels of *CIPK9* expression in wild-type (WT), *IDD10*, *idd10/CIPK9 OX* and *CIPK9 OX* determined using qRT–PCR. Levels of *CIPK9* mRNA were normalized against the level of *UBIQUITIN* mRNA in the same samples. Data are means ± S.E. ($n = 3$); different letters indicate significant differences between results ($P < 0.05$). (B) Appearances of wild-type (WT), *idd10*, *idd10/CIPK9 OX* and *CIPK9 OX* seedlings after growth for 4 d in a nutrient solution with either NO_3^- or NH_4^+ as the sole N source (Supplementary data Table S1). Scale bar = 1 cm. (C) Measurements of primary root length of plants grown as in (B). (D) Levels of cellular NH_4^+ levels in roots of seedlings grown for 4 d in a nutrient solution with either NO_3^- or NH_4^+ as the sole N source. Data shown in (C) and (D) are means ± s.e. ($n > 10$ plants per line); different letters indicate significant differences between results ($P < 0.05$).

mutants showed the same response to MSX (Supplementary data Fig. S12); NH_4^+-dependent retardation of root elongation could be rescued in both mutants by MSX treatment. The genetic interaction between *CIPK9* and *IDD10* was examined by overexpressing *CIPK9* in the *idd10* mutant background. The genetic data implied that either *CIPK9* acted downstream of *IDD10* in the signalling pathway or that *CIPK9* was required for the action of *IDD10* on ammonium-mediated root growth. All our data indicate that *CIPK9* and *IDD10* are involved in the same mechanisms regulating ammonium-mediated root growth.

It is well known that a high concentration of exogenous ammonium has a detrimental effect on plant growth and development (for reviews, see Britto and Kronzucker, 2002; Esteban *et al.*, 2016). Severe modifications in root architecture, including primary root systems, are widely recognized as an initial phenotypic symptom of NH_4^+ toxicity. Although we have demonstrated that *IDD10* and *CIPK9* work co-operatively to determine root growth in response to NH_4^+, the underlying cause of growth defects in their mutants in the presence of NH_4^+ remains unknown. The mutants showed lower NH_4^+ uptake activity and accumulated lower levels of cellular NH_4^+ than wild-type plants. This observation contrasts with the general notion that a high level of cellular ammonium is one of the major causes of NH_4^+ toxicity in higher plants.

Many physiological and molecular causes of NH_4^+-associated defects in roots have been suggested and discussed (for reviews, see Britto and Kronzucker, 2002; Esteban *et al.*, 2016). Given that low levels of cellular NH_4^+ accumulated in roots of *idd10* and *cipk9* mutants, increased NH_4^+ efflux resulting in excessive energy consumption might be one of the causes underlying their NH_4^+-associated phenotypes. Although the futile transmembrane NH_4^+ cycle hypothesis, which states that NH_4^+ exclusion from the cytoplasm eventually leads to growth retardation (Britto and Kronzucker, 2002), has been questioned (Esteban *et al.*, 2016), it would be worth examining whether NH_4^+ efflux increases in *cipk9* plants.

Another factor influencing NH_4^+ flux is the cellular K^+ concentration in roots. In arabidopsis, addition of potassium partially suppresses the retardation of root growth induced by NH_4^+ toxicity (Cao *et al.*, 1993). To examine whether potassium modulated the NH_4^+-associated root phenotypes of *cipk9* and *idd10*, the effect of potassium on growth of *cipk9*, *idd10*, *CIPK9 OX* and *idd10/CIPK9 OX* roots was examined (Supplementary data

Figs. S13 and S14). Potassium supplementation had no effect on root growth inhibition induced by NH_4^+ in either mutant.

Further study is required to understand the molecular nature of NH_4^+-associated root growth defects. Signalling responses to NH_4^+ have been extensively reported (for a review, see Esteban *et al.*, 2016). As *IDD10* and *CIPK9* encode a transcriptional regulator and a component of Ca^{2+} signalling modules, respectively, it is likely that the phenotypes observed in their mutants result from disruption of the signalling pathways involved in NH_4^+ tolerance. It is worth noting that $^{15}NH_4^+$ influx in *CIPK9 OX* was lower than that in wild-type plants but higher than that in *cipk9*. This implies that overaccumulation of *CIPK9* might have a dominant negative effect in the regulation of downstream signalling. In other words, the role of *CIPK9* might be fine-tuning $^{15}NH_4^+$ flux in rice root cells. A recent study of arabidopsis showed that *CIPK23* inhibits the activities of ammonium transporters by direct phosphorylation (Straub *et al.*, 2017). Ammonium uptake increased in arabidopsis *cipk23* mutants, but the opposite observation was made in *cipk9* mutants in this study. Although it is possible that CIPK9 performs enzymatic modification of ammonium transporters, the functional relationships between *CIPK*s and *AMT*s in rice may differ from those in arabidopsis.

Conclusion

This study demonstrated that *CIPK9* is a regulator of NH_4^+-dependent root growth in rice. Extensive analyses of transcriptomes and metabolomes are required to understand the molecular and physiological roles of *IDD10* and *CIPK9* in regulating root growth in response to NH_4^+. These results provide an important foundation for a more extensive understanding of the regulatory basis of NH_4^+ signalling in rice plants.

SUPPLEMENTARY DATA

Supplementary data are available online at https://academic.oup.com/aob and consist of the following. Table S1: modified half-strength KB nutrient solutions (pH 5.8). Table S2: modified half-strength KB with MSX (Fig. S12). Table S3: modified half-strength KB to examine K^+ effect (Figs S13 and 14). Table S4: sequences of primers used for qRT–PCR. Table S5: sequences of primers used in EMSA, ChIP and transient transfection assays. Figure S1: induction and purification of recombinant IDD10 protein. Figure S2: expression levels of (A) *AMT1;2* mRNA and (B) *IDD10* mRNA in *idd10*, *AMT1;2 OX4* and *idd10*/*AMT1;2 OX4* roots. Figure S3: chlorophyll content in shoots and primary root growth following exposure to different concentrations of NO_3^- or NH_4^+. Figure S4: responses of 12 *CIPK* genes (*CIPK3*, *5*, *8*, *9*, *10*, *11*, *12*, *14/15*, *23*, *24* and *31*) to NH_4^+. Figure S5: responses of ten *CBL* genes to NH_4^+ treatment. Figure S6: responses of five *CIPK* genes in roots of *idd10* and *IDD10 OX2* plants to exposure to NH_4^+. Figure S7: activation of *CIPK* promoters by IDD10. Figure S8: expression of *CIPK* genes in their respective insertion mutants. Figure S9: *CIPK9* expression patterns. Figure S10: selection and analysis of revertants from plants regenerated from *CIPK9::Ds* via tissue culture. Figure S11: levels of *AMT1;2* mRNA expression in wild-type (WT), *idd10*, *cipk9*, Rev. and *CIPK9 OX* plants. Figure S12: effect of MSX treatment on root growth of *idd10* and *cipk9*. Figure S13: effect of K^+ on NH_4^+-sensitive root growth of *idd10* and *cipk9*. Figure S14: effect of K^+ on NH_4^+-sensitive root growth of the *idd10*/*CIPK9 OX* genotype.

ACKNOWLEDGEMENTS

This research was supported by grants from the Basic Science Research Program through the National Research Foundation of Korea (NRF) funded by the Ministry of Education (2017R1D1A1B03030555), from the Next-Generation BioGreen 21 Program (PJ01326601), the Rural Development Administration, Republic of Korea, and from Natural Science Foundation of Liaoning Province (20170540812).

LITERATURE CITED

Abiko T, Obara M, Ushioda A, Hayakawa T, Hodges M, Yamaya T. 2005. Localization of NAD-isocitrate dehydrogenase and glutamate dehydrogenase in rice roots: candidates for providing carbon skeletons to NADH-glutamate synthase. *Plant & Cell Physiology* **46**: 1724–1734.

Bleckmann A, Weidtkamp-Peters S, Seidel CA, Simon R. 2010. Stem cell signaling in Arabidopsis requires CRN to localize CLV2 to the plasma membrane. *Plant Physiology* **152**: 166–176.

Brady SM, Burow M, Busch W, *et al.* 2015. Reassess the t test: interact with all your data via ANOVA. *The Plant Cell* **27**: 2088–2094.

Britto DT, Kronzucker HJ. 2002. NH_4^+ toxicity in higher plants: a critical review. *Journal of Plant Physiology* **159**: 567–584.

Cai H, Lu Y, Xie W, Zhu T, Lian X. 2012. Transcriptome response to nitrogen starvation in rice. *Journal of Bioscience* **37**: 731–747.

Cao Y, Glass AD, Crawford NM. 1993. Ammonium inhibition of Arabidopsis root growth can be reversed by potassium and by auxin resistance mutations aux1, axr1, and axr2. *Plant Physiology* **102**: 983–989.

Chin HG, Choe MS, Lee SH, *et al.* 1999. Molecular analysis of rice plants harboring an Ac/Ds transposable element-mediated gene trapping system. *The Plant Journal* **19**: 615–623.

Engelsberger WR, Schulze WX. 2012. Nitrate and ammonium lead to distinct global dynamic phosphorylation patterns when resupplied to nitrogen-starved Arabidopsis seedlings. *The Plant Journal* **69**: 978–995.

Esteban R, Ariz I, Cruz C, Moran JF. 2016. Review: Mechanisms of ammonium toxicity and the quest for tolerance. *Plant Science* **248**: 92–101.

Hirano T, Satoh Y, Ohki A, Takada R, Arai T, Michiyama H. 2008. Inhibition of ammonium assimilation restores elongation of seminal rice roots repressed by high levels of exogenous ammonium. *Physiologia Plantarum* **134**: 183–190.

Ho CH, Lin SH, Hu HC, Tsay YF. 2009. CHL1 functions as a nitrate sensor in plants. *Cell* **138**: 1184–1194.

Hsieh PH, Kan CC, Wu HY, Yang HC, Hsieh MH. 2018. Early molecular events associated with nitrogen deficiency in rice seedling roots. *Scientific Reports* **8**: 12207. doi: 10.1038/s41598-018-30632-1.

Hu HC, Wang YY, Tsay YF. 2009. AtCIPK8, a CBL-interacting protein kinase, regulates the low-affinity phase of the primary nitrate response. *The Plant Journal* **57**: 264–278.

Ishikawa-Sakurai J, Hayashi H, Murai-Hatana M. 2014. Nitrogen availability affects hydraulic conductivity of rice roots possibly through changes in aquaporin gene expression. *Plant and Soil* **379**: 289–300.

Jain M, Nijhawan A, Tyagi AK, Khurana JP. 2006. Validation of housekeeping genes as internal control for studying gene expression in rice by quantitative real-time PCR. *Biochemical and Biophysical Research Communications* **345**: 646–651.

Je BI, Piao HL, Park SJ, *et al.* 2010. RAV-Like1 maintains brassinosteroid homeostasis via the coordinated activation of BRI1 and biosynthetic genes in rice. *The Plant Cell* **22**: 1777–1791.

Kim CM, Piao HL, Park SJ, *et al.* 2004. Rapid, large-scale generation of *Ds* transposant lines and analysis of the Ds insertion sites in rice. *The Plant Journal* **39**: 252–263.

Kim JG, Li X, Roden JA, *et al.* 2009. Xanthomonas T3S effector XopN suppresses PAMP-triggered immunity and interacts with a tomato atypical receptor-like kinase and TFT1. *The Plant Cell* **21**: 1305–1323.

Kurusu T, Hamada J, Nokajima H, *et al.* 2010. Regulation of microbe-associated molecular pattern-induced hypersensitive cell death, phytoalexin production, and defense gene expression by calcineurin B-like protein-interacting protein kinases, OsCIPK14/15, in rice cultured cells. *Plant Physiology* **153**: 678–692.

Lanquar V, Loqué D, Hörmann F, *et al.* 2009. Feedback inhibition of ammonium uptake by a phospho-dependent allosteric mechanism in Arabidopsis. *The Plant Cell* **21**: 3610–3622.

Li J, Long Y, Qi GN, Xu ZJ, Wu WH, Wang Y. 2014. The OsAKT1 channel is critical for K^+ uptake in rice roots and is modulated by the rice CBL1–CIPK23 complex. *The Plant Cell* **26**: 3387–3402.

Lian X, Wang S, Zhang J, *et al.* 2006. Expression profiles of 10,422 genes at early stage of low nitrogen stress in rice assayed using a cDNA microarray. *Plant Molecular Biology* **60**: 617–631.

Liu LL, Ren HM, Chen LQ, Wang Y, Wu WH. 2012. A protein kinase CIPK9 interacts with calcium sensor CBL3 and regulates K^+ homeostasis under low-K^+ stress in Arabidopsis. *Plant Physiology* **161**: 266–277.

Ogasawara H, Kaimi R, Colasanti J, Kozaki A. 2011. Activity of transcription factor JACKDAW is essential for SHR/SCR-dependent activation of SCARECROW and MAGPIE and is modulated by reciprocal interactions with MAGPIE, SCARECROW and SHORT ROOT. *Plant Molecular Biology* **77**: 489–499.

Oliveira IC, Brears T, Knight TJ, Clark A, Coruzzi GM. 2002. Overexpression of cytosolic glutamine synthetase. Relation to nitrogen, light, and photorespiration. *Plant Physiology* **129**: 1170–1180.

Pandey GK, Cheong YH, Kim BG, Grant JJ, Li L, Luan S. 2007. CIPK9: a calcium sensor-interacting protein kinase required for low-potassium tolerance in Arabidopsis. *Cell Research* **17**: 411.

Patterson K, Cakmak T, Cooper A, Lager I, Rasmusson AG, Escobar MA. 2010. Distinct signalling pathways and transcriptome response signatures differentiate ammonium- and nitrate-supplied plants. *Plant, Cell & Environment* **33**: 1486–1501.

Shimizu H, Tanabata T, Xie X, *et al.* 2009. Phytochrome-mediated growth inhibition of seminal roots in rice seedlings. *Physiologia Plantarum* **137**: 289–297.

Sonoda Y, Ikeda A, Saiki S, Yamaya T, Yamaguchi J. 2003. Feedback regulation of the ammonium transporter gene family AMT1 by glutamine in rice. *Plant & Cell Physiology* **44**: 1396–1402.

Straub T, Ludewig U, Neuhaeuser B. 2017. The kinase *CIPK23* inhibits ammonium transport in *Arabidopsis thaliana*. *The Plant Cell* **29**: 409–422.

Wang W, Hu B, Yuan D, *et al.* 2018. Expression of the nitrate transporter gene *OsNRT1.1A/OsNPF6.3* confers high yield and early maturation in rice. *The Plant Cell* **30**: 638–651.

Wu Y, Yang W, Wei J, Yoon H, An G. 2017. Transcription factor *OsDOF18* controls ammonium uptake by inducing ammonium transporters in rice roots. *Molecules and Cells* **40**: 178–185.

Xu J, Li HD, Chen LQ, Wang Y, Liu LL, He L, Wu WH. 2006. A protein kinase, interacting with two calcineurin B-like proteins, regulates K^+ transporter *AKT1* in Arabidopsis. *Cell* **125**: 1347–1360.

Xuan YH, Priatama RA, Huang J, *et al.* 2013. Indeterminate domain 10 regulates ammonium-mediated gene expression in rice roots. *New Phytologist* **197**: 791–804.

Yamaguchi M, Ohtani M, Mitsuda N, *et al.* 2010. VND-INTERACTING2, a NAC domain transcription factor, negatively regulates xylem vessel formation in Arabidopsis. *The Plant Cell* **22**: 1249–1263.

Yang SY, Hao DL, Song ZZ, Yang GZ, Wang L, Su YH. 2015. RNA-Seq analysis of differentially expressed genes in rice under varied nitrogen supplies. *Gene* **555**: 305–317.

Yang W, Yoon J, Choi H, Fan Y, Chen R, An G. 2015. Transcriptome analysis of nitrogen-starvation-responsive genes in rice. *BMC Plant Biology* **15**: 31.

Yoo SD, Cho YH, Sheen J. 2007. Arabidopsis mesophyll protoplasts: a versatile cell system for transient gene expression analysis. *Nature Protocols* **2**: 1565–1572.

Yang HC, Kan CC, Hung TH, *et al.* 2017. Identification of early ammonium nitrate-responsive genes in rice roots. *Scientific Reports* **7**: 16885. doi: 10.1038/s41598-017-17173-9.

Yuan L, Loque D, Ye F, Frommer WB, von Wiren N. 2007. Nitrogen-dependent posttranscriptional regulation of the ammonium transporter AtAMT1;1. *Plant Physiology* **143**: 732–744.

Yuan L, Gu R, Xuan Y, *et al.* 2013. Allosteric regulation of transport activity by heterotrimerization of Arabidopsis ammonium transporter complexes *in vivo*. *The Plant Cell* **25**: 974–984.